Primljen / Received: 29.11.2021.
Ispravljen / Corrected: 29.5.2022.
Prihvaćen / Accepted: 12.6.2022.
Dostupno online / Available online: 10.7.2022.

Seismic response of post-tension shear walls – Outrigger structure

Authors:

Prof. **Mohamed Husain**, PhD. CE
Zagazig University, Zagazig, Egypt
Faculty of Engineering, Structural Engineering Department
Mo_husain2000@yahoo.com

Prof. **Hilal Hassan**, PhD. CE
Zagazig University, Zagazig, Egypt
Faculty of Engineering, Structural Engineering Department
hilalcivil@yahoo.com

Prof. **Heba A. Mohamed**, PhD. CE
Zagazig University, Zagazig, Egypt
Faculty of Engineering, Structural Engineering Department
hebawahbe@yahoo.com

Eman Saeed Elgharbawy, MCE
Higher Institute of Engineering and Technology, Belbeis, Egypt
em412019@gmail.com
Corresponding author

Research Paper

Mohamed Husain, Hilal Hassan, Heba A. Mohamed, Eman Saeed Elgharbawy

Seismic response of post-tension shear walls – Outrigger structure

This research was conducted by combining two structural systems: post-tensioned core walls and an outrigger in a 40-story building. A Vierendeel outrigger system was applied to one and two stories, and a comparison between models was performed to determine the best outrigger locations. In addition, the effect of post-tensioned core walls at only 25 % of the building height was investigated. Subsequently, the best positions of the Vierendeel outrigger system were applied with bonded post-tension core walls at a building height of only 25 %. The results showed an improvement in lateral stiffness using the outrigger, and roof displacement was enhanced by approximately 42 %. The post-tension core walls enhanced roof displacement by approximately 14 %. Both systems worked together to reduce roof displacement by approximately 50 %.

Key words:
Outrigger system, post-tension shear walls, time history earthquake, seismic response, Midas-Gen software program

Prethodno priopćenje

Mohamed Husain, Hilal Hassan, Heba A. Mohamed, Eman Saeed Elgharbawy

Seizmički odgovor naknadno prednapetih posmičnih zidova – Outrigger sustava ukruta

Ovo je istraživanje nastalo kao kombinacija dvaju konstrukcijskih sustava, a to su naknadno prednapeti zidovi jezgre i sustav ukrute (Outrigger) u zgradi sa 40 katova. Primijenjen je Vierendeelov sustav ukrute na jednom katu i na dva kata te su uspoređeni modeli kako bi se saznali najbolji položaji ukrutnih sustava. Jednako tako, proučen je utjecaj naknadno prednapetih zidova jezgre na samo 25 % visine zgrade. Usvojen je najbolji položaj Vierendeelovih sustava ukrute s naknadno prednapetim zidovima jezgre na samo 25 % visine zgrade. Rezultati su pokazali poboljšanje lateralne krutosti uporabom sustava ukrute, a pomak vrha se umanjio za 42 %. Utjecaj naknadno prednapetih zidova jezgre na umanjenje pomaka vrha je 14 %. Utjecaj oba sustava na umanjenje pomaka vrha je 50 %.

Ključne riječi:
sustav ukrute (outrigger), naknadno prednapeti posmični zidovi, vremenski zapis potresa, seizmički odgovor

1. Introduction

Tall buildings, particularly skyscrapers, have their own developmental structural systems that differ from ordinary structural systems. When lateral loadings act on the building, the building behaves as a cantilever fixed at the base. As the height increases, the cantilever deformation shape increases, giving a great base moment [1, 2]. Based on this, the internal core and shear walls have no capacity to meet top drift demand and cannot reduce the inter-story drift. This necessitates either increasing the inner core dimensions or increasing the number of shear walls, both of which are unlikely to reduce seismic damage and are costly. Thus, the ideal solution would be to use developmental structural systems, such as outrigger systems and post-tension concrete.

An outrigger system is an important system for enhancing seismic resistance of tall buildings and reducing seismic damage. The outrigger system helps operate the outer columns with the inner central core by connecting them. When lateral loads cause moment and rotation of the central core, these forces move the outrigger up and down, but the outer columns control this movement and generate opposite forces. These forces help change the direction of the outrigger movement and generate a reverse story shear in the core, which reduces the core moment and rotation [3].

2. Overview of previous outrigger and post-tension research

Previous researchers have studied outrigger systems, such as steel bracing or concrete deep beams. The outrigger story varies across the entire height of the building when one, two, and three stories are used to determine the best outrigger story for seismic resistance [4, 5]. Khandelwal and Singh [6] studied the steel outrigger seismic behavior in shape belt truss systems [X, V, and M] and carried out a comparison between the three shapes in multiple locations over the entire height of the building. To identify the position of the pest, a one-belt truss outrigger system was used at different positions on the 10th, 15th, and top floors of a 30-story building. In addition, a double-belt truss was applied in a 45-story building on the 15th and 30th stories, and a triple-belt truss was applied in a 60-story building on the 15th, 30th, and 45th stories. All models had the same dimensions, with a square plan of 35 × 35 m. The behavior of the models was studied using the response spectrum analysis method using the E-tabs software. They based their research results on maximum displacement, story drift, and rotation values. From the analysis, they concluded that the X-shaped belt truss outrigger system was the most efficient steel outrigger shape. The best position for the single outrigger system was at 0.5H, or on the 15th story. When the number of outriggers increases, the strength of the building increases because the triple outrigger provides the best control in the range of 33.69 %. Gawate et al. [7] expanded this research by determining the optimal outrigger story when used as a deep beam in a building with a total height of 111 m. They applied the outrigger system to one- and two-stories in two cases. In the first case, one outrigger was fixed at the 28th story, and the other was fixed throughout the height. In the other case, the two outriggers were 0.333H apart from one another. The seismic responses of the models were studied via response spectrum analysis using the E-tabs software program. They based their research results on the story drift parameter. All the models had a square plan, and they considered changes in columns and shear wall sizes. From the analysis, they found that 0.47H is the best location for a single outrigger system. 0.3H and H were the best outrigger locations in the first case, and 0.333H and 0.666H were the best locations in the second case.

Post-tensioned concrete is an appropriate system for increasing the strength of tall buildings to satisfy earthquake demands. Previous researchers have investigated the effect of post-tension tendons in beams and slabs, but only a few have recently investigated the effectiveness of post-tension tendons in shear walls. The post-tension shear wall is created by placing a very narrow duct with a diameter slightly greater than the diameter of the tendons that are inserted into it. After pouring concrete, the strands are tightened to the required strength using hydraulic devices and tied to the concrete at the foundations and roof floor using an end anchor. This method can be bonded or unbonded. The stresses are transferred by the end bearing, not by bonding, when the cable curves through the radial pressure between the cable and the duct in unbonded post-tension, unlike the bonded post-tension [8]. Stevenson, M., Panian, L., Korolyk, M., and Mar, D. [9] demonstrated the post-tension technique, and provided evidence and photos from the site, which was a 4-story office building with a post-tension C-shaped central core and post-tension slab. Post-tension tendons were applied to the core flange. The tendons were installed via a block-out at the base level of the walls, as shown in Figure 1.a. After stressing the strands using a single multistrand hydraulic jack, as shown in Figure 1.b, the block-out was poured and all the walls became solid.

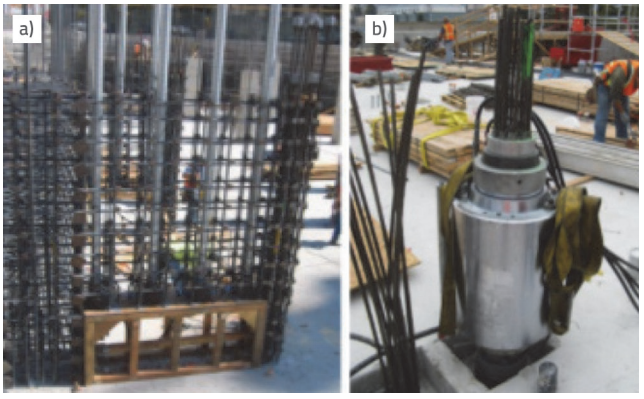

Figure 1. a) The anchorage block-out at the base of PT core; b) Single multi-strand hydraulic jack [9]

Shatnawi et al. [10] investigated the seismic behavior of post-tensioned shear walls and observed a large lateral deformation of buildings without failure. They compared the behavior of five types of concrete shear walls under lateral cyclic loads using the ABAQUS program. The first type of wall (wall A) was an ordinary wall or a wall with mild steel support and without post-tension tendons. Three types of walls were hybrid post-tensioned shear walls with a constant number of tendons, but the variation was in the post-tension steel and mild steel areas. The tendon specifications were grade 270 with seven-wire strands and their properties were according to ASTM [11]. The last type was a wall with post-tension wires and no mild steel. Each wall model was applied to a six-story building model with a plan dimension of 30 m × 27 m and a total height of 18 m. The research results were based on five limit states observed on the base shear-roof drift figure for the five walls, which were base wall decompression, yielding mild and post-tension steel, influent base shear-roof drift relationship in the linear limit, and concrete crushing. From the analysis, they discovered that the unbonded post-tension shear wall exhibited a large nonlinear lateral drift but without the tendons yielding. The elasticity was reduced when the steel-bar area of the PT reinforcement was increased. It was also observed that when the ratio between the post-tension and mild steel areas increased, the base shear at decompression increased. However, the base shear values reduced at the yielding of mild steel; the permanent deformation reduced and the capacity improved.

3. Methodology

The aim of our research was to combine the two systems, i.e., the outrigger and the post-tension shear walls, and apply the combination to a 40-story building to test whether such a system can protect tall buildings in the event of an earthquake with minimal damage. The seismic behavior was studied using a nonlinear dynamic procedure or the time history analysis method, which is the most accurate and reliable approach for seismic analysis. The building was subjected to real earthquake shaking, which was recorded using Midas, a design and analysis software:

1. A 40-story reference model with an ordinary structural system was drawn, and its materials were defined using the program MIDAS-GEN.
2. The dead load, live load, and 0.356 g El-Centro earthquake load were added.
3. The model was analyzed and the roof lateral displacement, drift index, fundamental period, and base moment were obtained as the model results.
4. The outrigger was added as a Vierendeel to the model on one or two floors by drawing beams tied to the central core walls and perimeter columns with posts in the middle, as shown in Figure 6.a and recommended in [12, 13].
5. The outrigger models were analyzed under the same permanent and lateral loads.
6. The reference and outrigger models were compared to choose the best position, and the results are shown in the figures and tables.
7. Bonded post-tension tendons were added to the central core walls in the first ten stories (25 % of the building height) at the boundaries of the walls by defining the tendon profile, tendon property, and post-tension force.
8. The post-tension model was analyzed under the same permanent and lateral loads.
9. A model combining both systems, applying the best locations of the Vierendeel outrigger and using bonded post-tension central core walls at only 25 % of the 40-story building height, was designed and analyzed under the same permanent and lateral loads as above.
10. The reference model was compared with the post-tension model and the model with the combined systems, and the results are shown in the figures.
11. The results were analyzed and conclusions were drawn.

4. Midas-Gen analysis program

Midas-Gen is an advanced finite element software that has several large datasets of approximately 30 earthquake records from 1940 to 1990. The user can export earthquake data to the program to study the effect of a real earthquake on a 3D tall building. The program can predict the large displacement behavior of 3D tall buildings by considering both geometric nonlinearities and material inelasticity. It also allows the analysis of post-tension concrete by defining the post-tension tendon materials, jacking force, and tendon profile shape, drawing the ducts inside sections, and considering the post-tension losses [14].

5. Verification

5.1. Verification with experimental work

To verify the accuracy of the seismic behavior analysis of the model, we simulated and analyzed the experimental work by Paul and Agarwal [15] in the Midas-Gen program and compared the program results with their experimental results. In 2012, Paul and Agarwal [15] experimentally tested a reinforced concrete frame without an infill wall under pushover seismic loading. The frame had a quarter-scale size with a height of 1200 mm and a span of 1260 mm, as shown in Figure 2.a. They used a servo-hydraulic actuator to load the frame slowly, which was fixed in the laboratory on a steel plate to reduce the strain on the material. LVDT arrangements were used to measure the capacity curve of the model under a pushover load, as shown in Figure 2.b [15]. The same model was studied in the Midas-Gen program under pushover seismic loading [16], which was performed according to the American Society of Civil Engineers (ASCE), and the load combination was added according to the [IS]

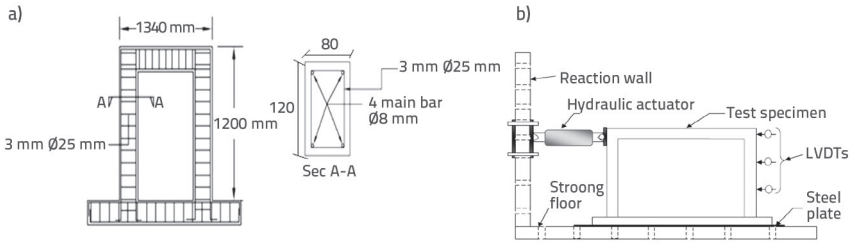

Figure 2. a) Reinforcement details of the lab model; b) loading setup of the lab model [15]

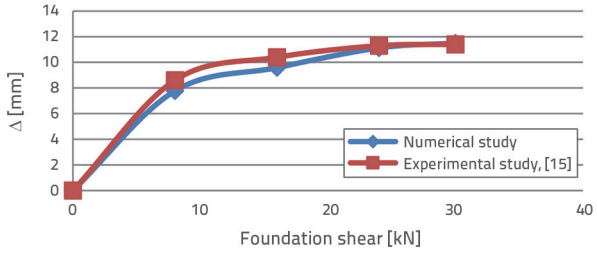

Figure 3. Comparison between simulations and experimentally obtained capacity curves by Paul and Agarwal [15]

Table 1. Experimental pushover capacity curve by Paul and Agarwal [15] and the corresponding numerically calculated values

Lateral force [kN]	Experimental displacement [mm]	Analytical displacement [mm]	Difference between values
0	0	0	0
8.2	8.6	7.8	9.5 %
16.3	10.4	9.6	7.8 %
24.5	11.3	11.1	1.5 %

code [17]. A comparison between the experimental and numerical capacity curves is presented in Figure 3 and Table 1, which show that the maximum difference between the values of the experimental and numerical capacity curves was 10 %. This indicates a good agreement between the simulation and actual results.

5.2. Verification with numerical work

Another comparison was performed with the numerical model of Kamath, K., Divya, N., and Rao, A. U. (2012) [18]. In 2012, Kamath, Divya, and Rao tested the effect of the El Centro earthquake with a PGA of 0.386 g on a 40-story high-rise building using the E-tabs program. The reference model was 140 m, with a typical floor height of 3.5 m. The area of the plan was 24 m × 27 m, with a central core of 7 m × 8 m and a thickness of 300 mm, as shown in Figure 4. The beams, columns, and core walls were assumed to be made of C250 concrete structures. The column and beam sizes considered in the analysis were 750 mm × 750 mm and 230 mm × 450 mm, respectively. We used the same model in the Midas-Gen program. A comparison between the two numerical models for the story displacement presented in Figure 5 and Table 2 shows that the maximum difference between the numerical story displacement values was 7.4 %.

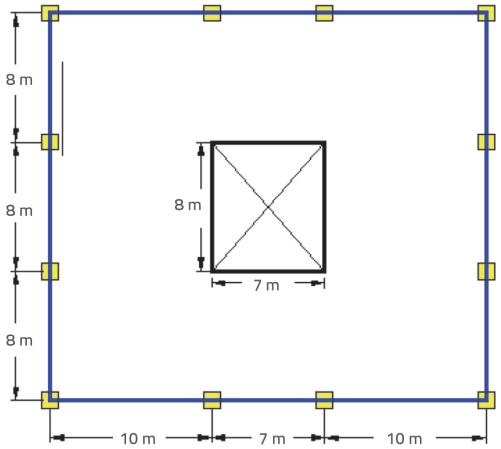

Figure 4. Model plan by Kamath, Divya, and Rao (2012) [18]

Table 2. Comparison between our numerical study and the results for story displacement values [18]

Story No	Numerical displacement [mm]	Displacement obtained in research Kamatha et al. [18] [mm]	Difference between values
15	231.4	250	7.4 %
20	338.2	350	3.4 %
25	474.1	500	5.2 %
30	611.2	625	2.2 %
40	914.2	950	3.8 %

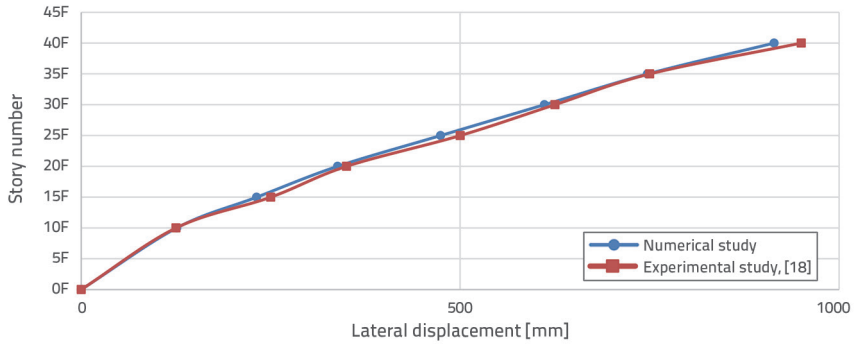

Figure 5. Comparison between the numerical study and the results for story displacement values [18]

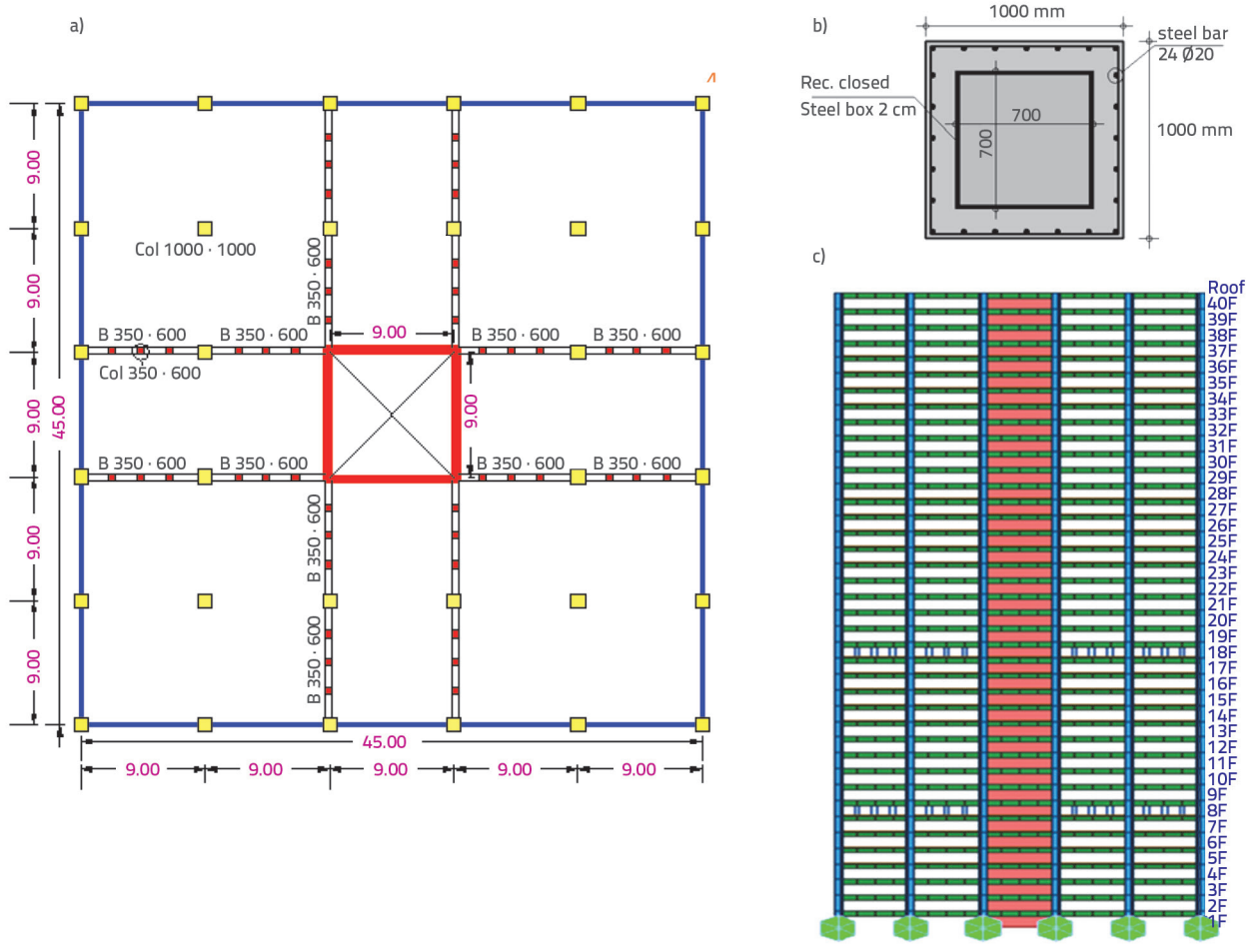

Figure 6. a) Vierendeel outrigger plan; b) composite column reinforcement detail; c) Elevation of model with outriggers at 8th and 18th stories

6. Model layout

The 40-story 3D models, described below, differed in the structural systems but had identical plan dimensions of 45 × 45 m. The plan was symmetrical, with a 9 m fixed dimension between the center of the columns and a square central core dimension of 9 × 9 m. The total height of the models was 120 m, and all stories were typical with a height of 3 m. Four materials were defined for the models: concrete, steel bars, composite materials, and high-strength PT steel. The material properties are listed in Table 4. The nonlinear behaviors of the materials as recommended in Midas-Gen, shown in Figures 9 and 10, vary widely with the loading methods and material properties. The reinforcement ratio of each element was calculated and taken as a constant value for all the models according to the Egyptian reinforced concrete design code [19]. The model section sizes are listed in Table 3. The models are:

- An ordinary structural model system without an outrigger system and post-tension shear wall was considered as the reference model.
- Single-story outrigger models were applied as Vierendeel links between the core walls at the building center and the boundary columns, as shown in Figure 6.a. According to [12, 13], the Vierendeel outriggers were added to the 8th, 18th, 30th, and 40th stories. The Vierendeel outrigger dimensions are presented in Table 3.
- Two-story outrigger models were applied as a Vierendeel in the 8th and 18th, 8th and 30th, and 18th and 30th stories, as shown in Figure 6.c.
- Two-story outrigger models were applied as a Vierendeel in the 8th and 40th, 18th and 40th, and 30th and 40th stories.
- A model with bonded post-tension tendons was applied to the core walls at only 25 % of the 40-story building height. The bonded post-tension tendons were controlled and tied at the foundations and opening gaps or block-outs in the core wall sides on the 10th story using end anchors after pouring the building concrete, as shown in Figure 1.a.

The total area of the post-tension tendons was calculated according to Egyptian code [19] as:

$$A = \frac{p_{j \cdot 1000}}{\text{jacking stress}} = 52974 \text{ mm}^2$$

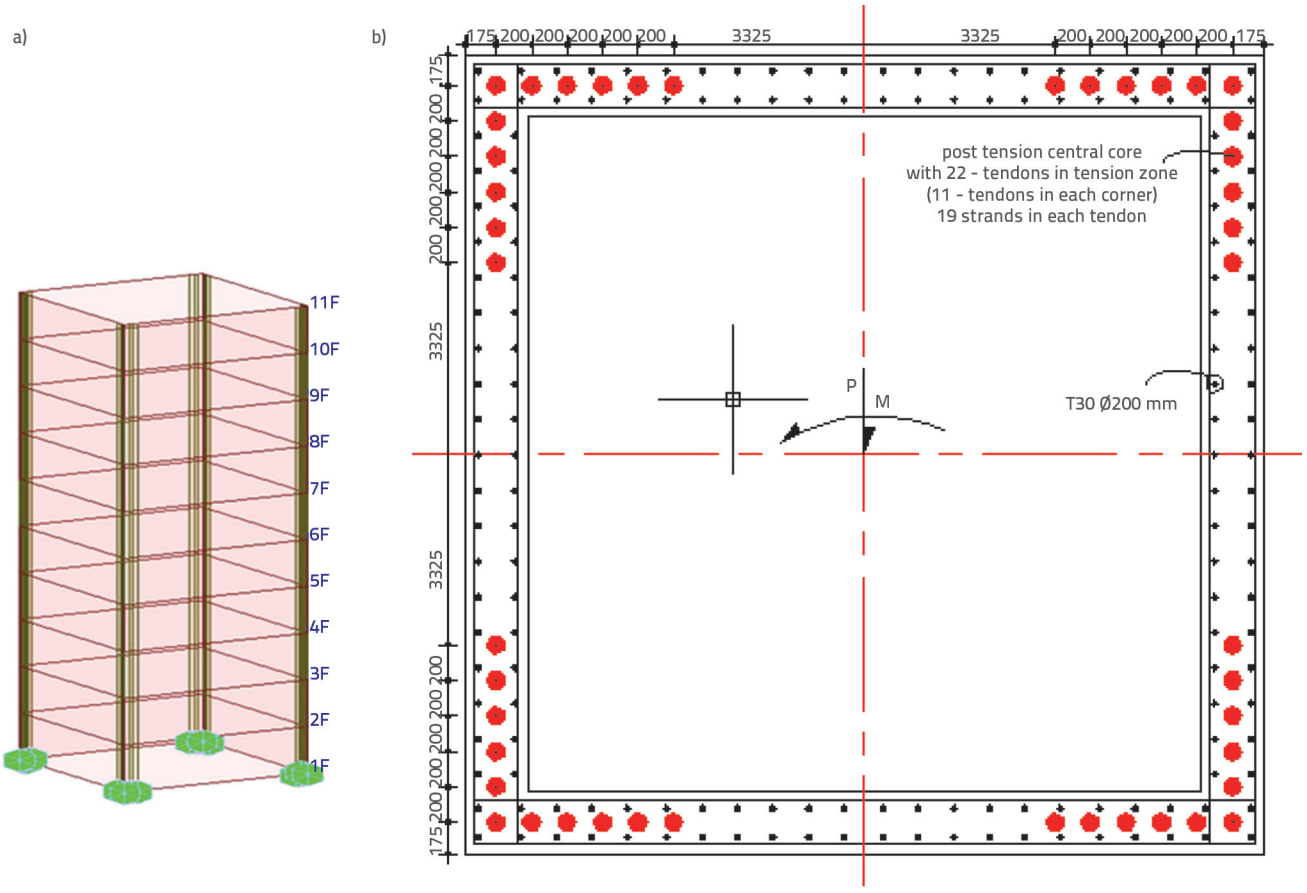

Figure 7. a) Elevation of 10-story core wall from 40-stories with straight post-tension tendons; b) post-tension core wall section reinforcement detail

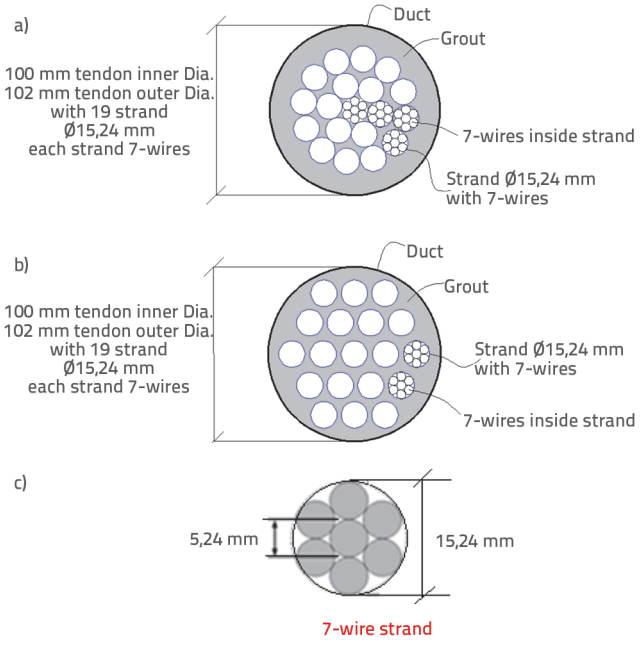

Figure 8. a, b) Cross-section of a tendon with 19 strands, each strand with 7 wires; c) Cross-section of a strand with 7 wires, each wire having a diameter of 5.24 mm

The tendons were placed straight inside the bonded ducts with inner and outer diameters of 100 and 102 mm, respectively. As shown in Figures 7.a and 7.b, 11 tendons were installed at each core corner. Each tendon has 19 strands, as shown in Figures 8.a and 8.b. The strand diameter was 15.24 mm, and each strand had seven wires, as shown in Figure 8.c. The ultimate strength and yield strength of the post-tension steel were 1860 and 1670 MPa, respectively.

A model with a combined structural system, using the best location for Vierendeel outriggers and post-tension tendons, was applied to the core walls at only 25 % of the 40-story building height.

Table 3. Section dimension of the numerical model in mm

Columns		Composite 1000 × 1000
Core thickness		350
Slab thickness		Flat 250
Boundary beams		300 × 900
Outrigger dimensions	**Vierendeel**	Beams 350 × 600
		Posts 350 × 600
	Deep beams	350 × 2700

Table 4. Material section propertiesSlika 10. Radni dijagram betona

Property	Concrete	Steel bar	Composite material	Post tension steel
Modulus of elasticity. E [MPa]	23503	200000	200000	190000
Poison's ratio. ν	0.200	0.303	0.303	0.303
Mass density [N/m^3]	24000	78600	78600	78600
Strength [MPa]	f_{cu} = 35	f_{py} = 400	f_{py} = 360	f_{py} = 1670
Strain	ε_{cu} = 0.003	ε_{cu} = 0.00207	ε_{cu} = 0.002	ε_{cu} = 0.00879

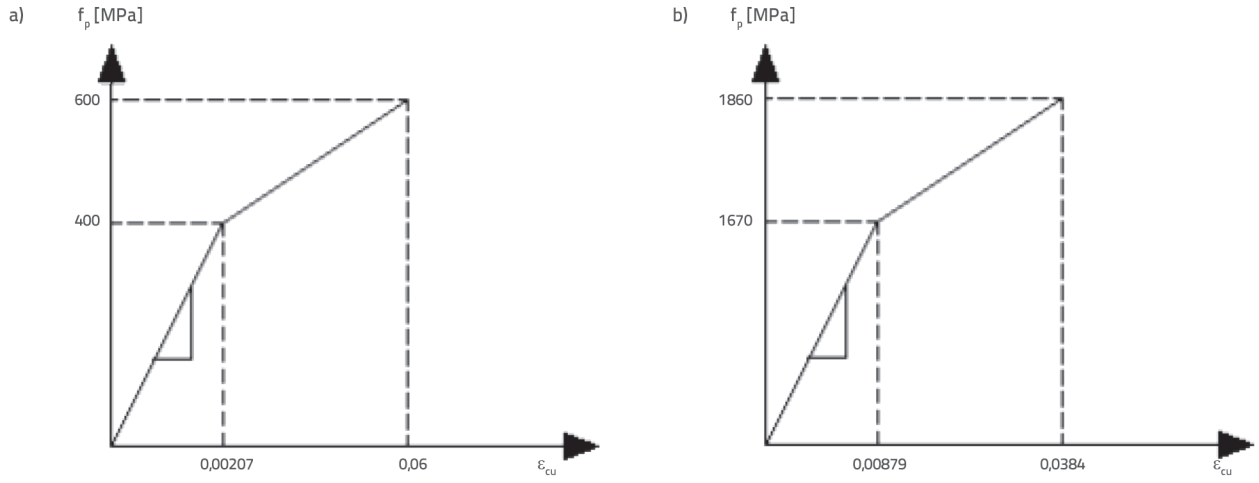

Figure 9. a) Nonlinear stress-strain curve of steel bars; b) nonlinear stress-strain curve of post-tensioned steel

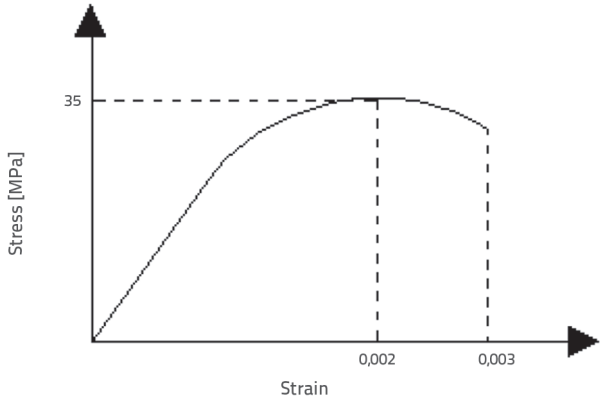

Figure 10. Nonlinear stress-strain curve of concrete

7. Loading

All models were studied under the same permanent and horizontal loads. The self-weight was added automatically by the program, and a live load of 2.5 kN/m^2 was added as a surface pressure load. The dynamic load effect was studied under a 0.356 g El Centro seismic load for 56 s. Additionally, the jacking post-tension force (was applied to the tendons in the post-tension wall models. The jacking post-tension force (and the post-tension force after the final losses were calculated according to the following fully tensioned stresses, one of which was at the service stage, as shown in Figure 11.

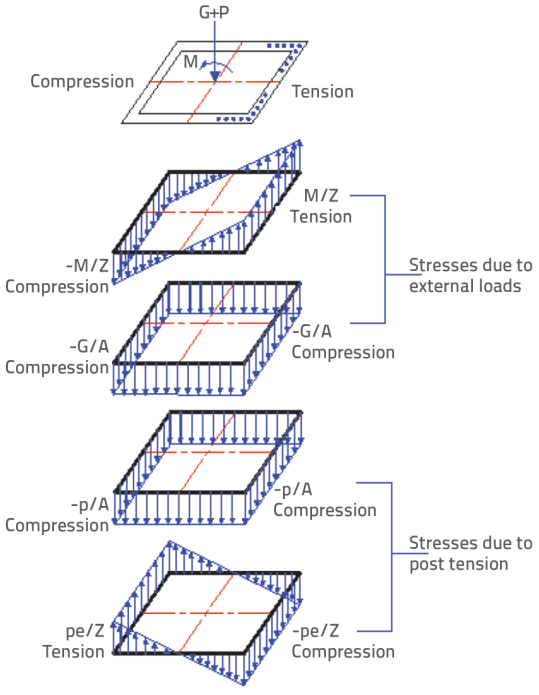

Figure 11. The stress distribution at the base of bonded post-tension core walls

Fully tensioned stress equation at service stage:

$$\left[\frac{-p_e}{A}-\frac{G}{A}\right]-\left[\frac{p_e \cdot e}{Z}\right]+\left[\frac{M}{Z}\right]=0 \quad (1)$$

P_e = 58627.16 kN

Jacking force, $Pj = \frac{p_e}{1- \% \text{ smanjenje}} = \frac{56992,32}{0,85} = 68973.13$ kN

where:

- G denotes the force on the core under gravity loads (dead + live loads), G = 122243.97 kN
- tension moment, M =696973.45 kN.m
- the area of the section, A = (9 × 0.35×2) + (2×0.35×8.3) = 12.11 m^2
- section elastic modulus, z = (I_x/Y) = (151.26/4.5)
- the eccentricity, e = 3.325 m

8. Results and discussion

The comparison between the numerical model's results is discussed as follows.

8.1. Stiffness and fundamental periods

Increasing the stiffness of tall buildings to minimize building damage under the seismic load effect is the main task of this study. The increase and decrease in the stiffness of the building were identified by determining the fundamental time of the building. When the natural period decreases, the building stiffness increases [20] as given by Eqs. (2) and (3):

$$T_n = 2\pi\sqrt{\frac{m}{K}} \quad (2)$$

$$K = \frac{F}{\delta} \quad (3)$$

where:

T_n - the fundamental period in which the building completes one vibration cycle in seconds under seismic loads

K - building stiffness or building resistance to deformation under seismic loads during the fundamental period

δ - building deformation or mode shapes of the building under seismic loads during the fundamental period.

The analyzed model had several mode shapes, and each mode shape occurred at a fundamental time. Following the analysis, the fundamental periods for the models in the first mode shape were recorded textually in the tables. The values in Tables 5 and 6 show that the fundamental periods of the model with a single outrigger at the 18th story and that with two outriggers at the 8th and 18th stories are the lowest among all models with the outrigger system. This indicates an increase in the lateral stiffness of the models. In addition, the values in Table 7 show that the building with the combined system has the lowest fundamental period and highest stiffness among all the models.

Table 5. Fundamental period of the single-story outrigger model

The model type	Time in seconds
Reference model	**5,99**
Outrigger @ 8th story	5,8
Outrigger @ 18th story	5,69
Outrigger @ 30th story	5,82
Outrigger @ roof story	5,92

Table 6. Fundamental period of models with outriggers at two stories

The model type	Time in seconds
Reference model	**5.99**
Outrigger @ (8th & 18th) stories	5.53
Outrigger @ (8th & 30th) stories	5.64
Outrigger @ (18th & 30th) stories	5.54
Outrigger @ (8th & 40th) stories	5.75
Outrigger @ (18th & 40th) stories	5.64
Outrigger @ (30th & 40th) stories	5.78

Table 7. Fundamental period of models with different structural systems

The model type	Time in seconds
Reference model	**5.99**
A model with post-tension in the central core only	5.81
A model with combined structural systems	5.38

8.2. Roof displacement

According to the Indian standard code (456:2000), [21], the allowable maximum displacement can be obtained from the relation: (building height from base to roof story)/500. Consequently, the allowable maximum displacement was 240 mm for a 120 m building height. The post-tension system is a structural system that helps reduce the effect of side loads on buildings by generating a moment opposite to the earthquake moment. This process helps increase the building strength and enhances the total building deformation under the seismic load effect.

In addition, the overall building lateral displacement was improved by using the core-outrigger system because it increases building stiffness. According to Eq. (3), the building deformation decreases when the building stiffness increases. The story lateral displacement for the models obtained from the analysis is presented in tables and plotted in figures for comparison with the reference story lateral displacement model.

The story lateral displacement values for the outrigger models are shown in Figures 12.a, 12.b, and 12.c and in Tables 8, 9, and 10. A comparison between the values indicated a roof displacement reduction of 41.98 % when the outrigger was installed at the 8th and 18th stories, and 25.3 % when the outrigger was installed in the 18th story, both relative to the reference model. For the other models, the reduction was between these two values. The story lateral displacement values for the different structural system models are shown in Figure 12.d and Table 11. A comparison between the values indicated a roof displacement reduction of 13.23 % when the post-tension steel was installed on the core walls at only 25 % of the building height. The roof displacement reduction reached 50 % for the combined structural system, which included an outrigger system at the 8th and 18th stories and bonded post-tension core walls at 25 % of the building height.

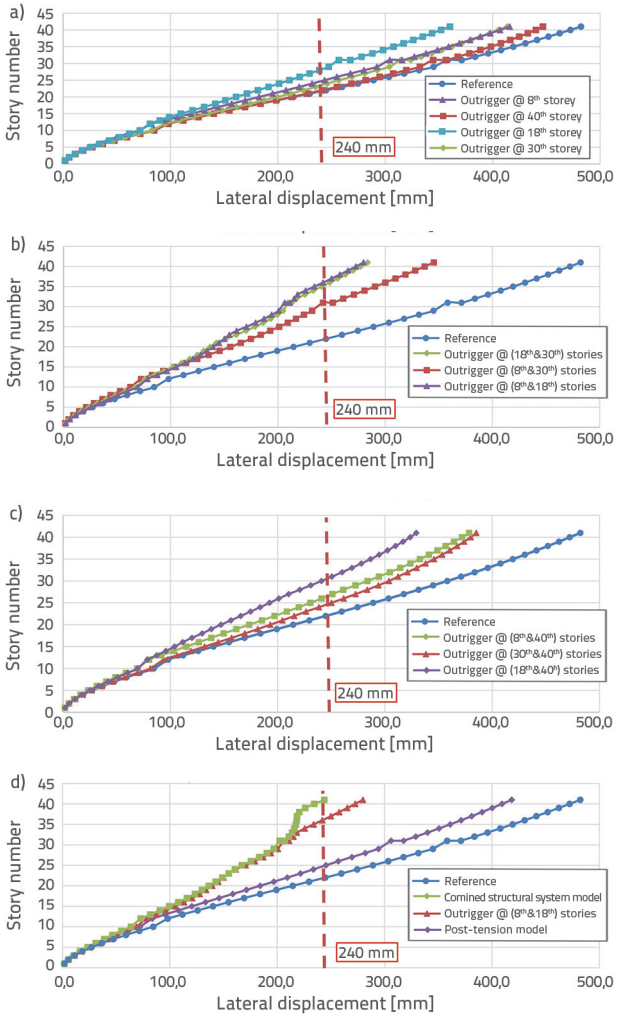

Figure 12. Story number vs. story lateral displacement for: a) single-story outrigger models; b) models with outrigger systems at two stories; c) models with outriggers at two stories, with one of them at the 40th story; d) models with different structural systems

Table 8. Roof story lateral displacement values in mm for single-story outrigger models

Type of structural system	Roof story drift [mm]
Reference model	482.2
Outrigger @ 8th story	415.8
Outrigger @ 18th story	360.2
Outrigger @ 30th story	413.5
Outrigger @40th story	446.7

Table 9. Roof story lateral displacement values in mm for models with outriggers at two stories

Type of structural system	Roof story drift [mm]
Reference model	482.2
Outrigger @ [8th & 18th] stories	279.8
Outrigger @ [8th & 30th] stories	345.4
Outrigger @ [18th & 30th] stories	283.7

Table 10. Roof story lateral displacement values in mm for models with outriggers at two stories, with one outrigger at the 40th story

Type of structural system	Roof story drift [mm]
Reference model	482.2
Outrigger @ (8th & 40th) stories	378.5
Outrigger @ (18th & 40th) stories	329.3
Outrigger @ (30th & 40th) stories	385.2

Table 11. Roof story lateral displacement values in mm for different structural systems

Type of structural system	Roof story drift [mm]
Reference model	482.2
Outrigger model @ (8th &18th) stories	279.8
Post tension model	418.4
Combined system model	243.8

8.3. Drift index

The allowable story drift can be calculated from the relation [0.005h], where h is the story height according to the Egyptian code [19]. This equation gives us the allowable story drift for a 3 m story height of 0.015.

The drift indices for the models were analyzed and plotted in figures with the reference drift index values. Figure 13 shows that for all stories, an overall improvement of 31.94 %, 37.14 %, 15.25 %, and 39.13 % are observed in the drift indices when the outrigger is applied at the 18th story, two outriggers are applied at the 8th and 18th stories, post-tension core walls are installed at only 25 % of the building height, and a combined structural system is used, in which two outriggers are applied at the 8th and 18th stories and post-tension core walls at 25 % of the building height, respectively.

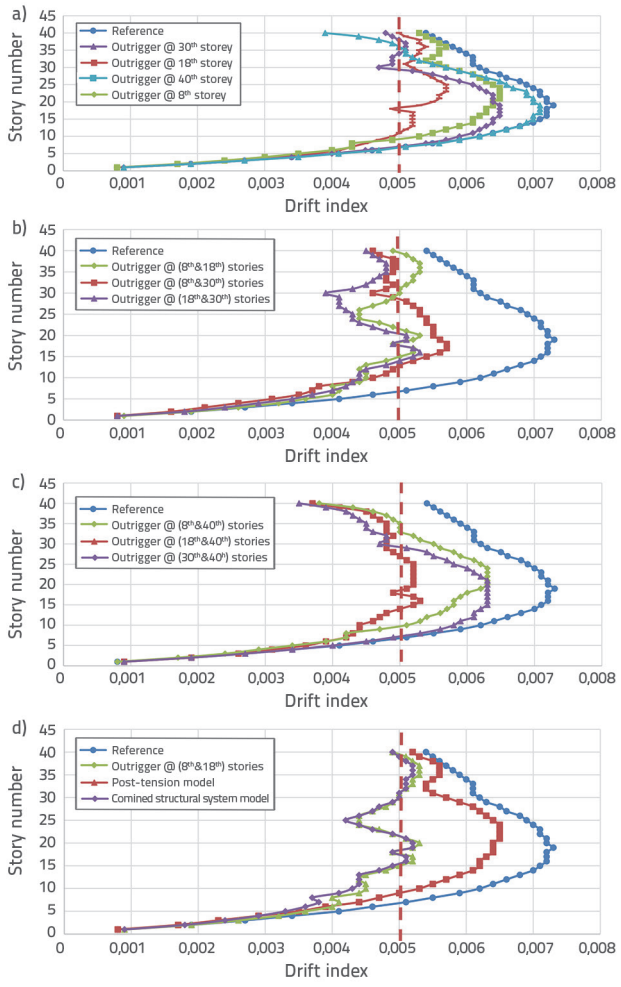

Figure 13. Story number vs. drift index of: a) single-story outrigger models; b) models with outriggers at two stories; c) models with outriggers at two stories, with one of them at the 40th story; d) models with different structural systems

8.4. The Base moment

A building without an outrigger system behaves like a cantilever system, and all the earthquake moments affect the central core. However, the outrigger system helps reduce the cantilever action of the building by connecting the walls of the central core with the columns at the building boundary. The core moments move to the boundary columns through the outriggers as horizontal forces. These forces turn into vertical forces in the columns such that the earthquake moment is reduced in the core building. In addition, post-tensioned concrete increases the stiffness of the building and reduces the core moment because the pre-stress force generates a moment opposite to the earthquake moment on the core. The base moment for each structural system is analyzed and plotted in a figure for comparison with the reference base moment model.

As shown in Figure 14 and Tables 12 and 13, the base moment was reduced.

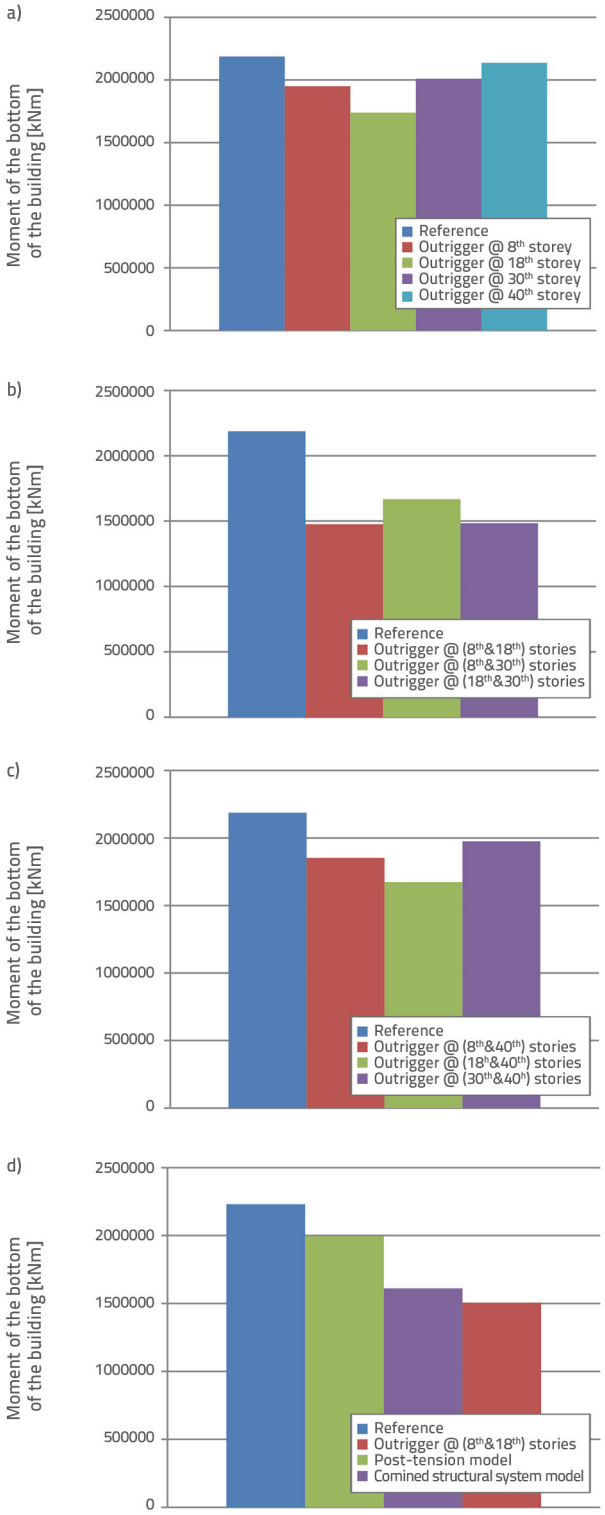

Figure 14. Base moment values for: a) single-story outrigger models; b) models with two outriggers; c) models with outriggers applied to two stories, with one of them at the 40th story; d) models with different structural systems

The moment of the bottom of the building decreased by 20.47 %, 32.53 %, 10.46 %, and 28 % compared with the reference

model when the outrigger was installed at the 18th story, two outriggers were installed at the 8th and 18th stories, post-tension steel was applied to only 25 % of the building height in the core walls, and the combined structural system was used, in which two outriggers were installed at 8th and 18th stories and post-tension core walls were applied in only 25 % of the building height, respectively.

Table 12. Base moment in kN.m for all outrigger models

Single outrigger models				
Ref.	**8th story**	**18th story**	**30th story**	**40th story**
2186920	1949510	1739170	2010120	2136350

Models with outriggers applied at two stories			
Ref.	**(8th & 18th) story**	**(8th & 30th)story**	**(18th & 30th) story**
2186920	**1475540**	**1667190**	1483360
	(8th & 40th) story	**(18th & 40th) story**	**(30th & 40th) story**
	1852060	1672850	1975110

Table 13. Base moment in kN.m for different structural system models

Type of structural system	Moment [kNm]
Reference model	2186920
Outrigger model @ (8th & 18th) stories	1475540
Post tension model	1958190
Combined system model	1575460

8.5. Base shear force

The base-story shear force may increase or decrease based on the distribution of the forces between the core and outrigger systems and depending on the relative stiffness of each element. In addition, there are parameters that affect the base shear force, such as the total weight of the building, natural time, and response reduction factor. The outrigger system increases the total weight of the building and reduces natural time, which helps to increase the base shear force value. However, the outrigger model increases the ductility of the building, which is proportional to the response reduction factor.

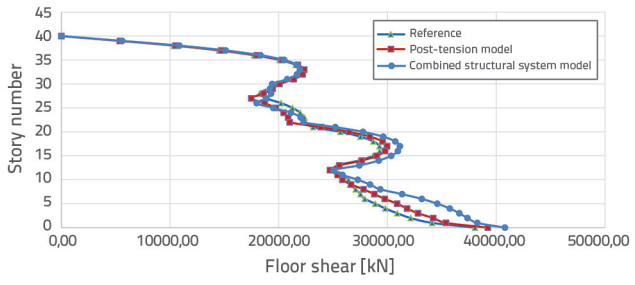

Figure 15. Variation in the base shear force for different structural systems

By contrast, the shear force is inversely proportional to the response reduction factor, indicating a reduction in the base shear value.

As shown in Figure 15 and Table 14, the base shear force increases by 3 % and 6.8 % when post-tension steel is applied to only 25 % of the building height in the core walls and the combined structural system is used, in which two outriggers are installed at the 8th and 18th stories and post-tension core walls are applied to only 25 % of the building height, respectively.

Table 14. Comparison between base shear force in kN for different structural systems

Type of structural system	Shear force [kN]
Reference model	38040
Post tension model	39226.00
Combined system model	40796.00

9. Conclusions

We studied the effectiveness of a combined structural system, which included the best locations of Vierendeel outriggers at the 8th and 18th stories, and wherein the post-tension core wall was applied to only 25 % of the 40-story tall building height. We also studied, through simulations, the effect of each system separately on a tall building when it was exposed to a strong earthquake. The seismic effect was studied by applying a 0.356 g El Centro seismic load for 56 s to the simulated tall building using the Midas-Gen program. Our research conclusions were based on the natural period, roof displacement, drift index, base shear force, and base moment as follows:

- The seismic behavior of the tall building was different for each structural system.
- Converting 25 % of the core wall height to post-tension helped improve the behavior of the tall building under seismic load compared to the reference model.
- The Vierendeel outrigger is a very effective system for improving the seismic behavior of tall buildings.
- Increasing the outrigger dimensions and the number of stories to which the outrigger is applied helped to increase the seismic resistance of tall buildings.
- The combined structural system proved to be more efficient in the reduction in roof displacement, drift index, base moment, and fundamental period because the stiffness of the tall building under seismic loads increased more than it did for each system separately.
- The roof displacement, drift index, and base moment improved relative to the reference model by 50 %, 39.13 %, and 28 %, respectively, when the combined structural system was used, in which Vierendeel outriggers were installed at the 8th and 18th stories and post-tension core walls were applied to only 10 stories of the 40-story tall building, i.e., up to 25 % of the building height.

REFERENCES

[1] Hallebrand, E., Jakobsson, W.: Structural design of high-rise buildings, TVSM-5000, 2016.

[2] Sundar, R.S., Gore. N.G.: Study on Tall RC Structure with Outrigger System Subjected to Seismic and Wind Loading, International Journal of Engineering Research & Technology, 6 (2017) 2, ISSN: 2278-0181.

[3] Rathore, A., Savita, M.: The behavior of outrigger structural system in high-rise building: reviews, International Journal of Science, Engineering and Technology Research, 6 (2017).

[4] Ahmed, J., Sreevalli, Y.: Application of Outrigger in Slender High Rise Buildings to Reduce Fundamental Time Period, 6th IRF International Conference, Chennai, India, July, 2014.

[5] Choi, H. S., Ho, G., Joseph, L., Mathias, N.: Introduction to Outrigger Systems - Outrigger Design for High-Rise Buildings, Routledge, 2017., pp.13–24, DOI: 10.1201/9781315661971-7

[6] Khandelwal, R., Singh, S.: Optimum Shape and Position of Outrigger System for High Rise Building under Earthquake Loading, Regular Issue, 9 (2020) 3, pp. 3268–3275, DOI: 10.35940/ijitee.c8961.019320.

[7] Gawate, Alpana L., Bhusari, J.P.: Behavior of Outrigger Structural System for High-rise Building, International Journal of Modern Trends in Engineering and Research, (2015), e-ISSN: 2349-9745.

[8] Kurama, Y.C.: Seismic Design of Partially Post-Tensioned Precast Concrete Walls, PCI Journal, 50 (2005) 4, pp.100–125, DOI: 10.15554/pcij.07012005.100.125

[9] Stevenson, M., Panian, L., Korolyk, M., Mar, D.: Post-tensioned concrete walls and frames for seismic-resistance-a case study of the David Brower Center, Seaoc 2008 Convention Proceedings, 2008., pp. 1-8

[10] Shatnawi, A., Abdallah, S.G., Tarawneh, B.: Seismic Behavior of Hybrid Post-Tensioned Cast in Place Concrete Shear Walls, Arabian Journal for Science and Engineering, 44 (2018) 5, pp. 4095 – 4109, DOI: 10.1007/s13369-018-3281-4

[11] American Society for Testing and Materials: Standard Specification for Steel Strand, Uncoated Seven-Wire for Pre-stressed Concrete, ASTM (A416/A416M – 12a), DOI: 10.1520/a0416_a0416m-12a

[12] Taranath, B.S.: Reinforced Concrete Design of Tall Buildings, 2009., DOI: 10.1201/9781439804810

[13] Taranath, B. S.: Wind and earthquake resistant buildings: Structural analysis and design, CRC press, 2004., DOI. 10.1201/9780849338090

[14] Midas, I. T.: Midas Gen on-line manual: general structure design system, MIDAS Information Technology, http://manual.midasuser.com/EN_Common/Gen/855/index.htm, 2017.

[15] Paul, G., Agarwal, P.: Experimental verification of seismic evaluation of RC frame building designed as per previous IS codes before and after retrofitting by using steel bracing, Asian Journal of Civil Engineering (Building and Housing), 13 (2012) 2, pp. 165-79

[16] FEMA 356: Pre-standard and Commentary for the Seismic Rehabilitation of the Buildings, Federal Emergency Management Agency & American Society of Civil Engineers, 2000.

[17] BIS, I.: Indian Standard Criteria for Earthquake Resistant Design of Structures, Bureau of Indian Standards (5th Revision), New Delhi, 2002.

[18] Kamath, K., Divya, N., Rao, A.U.: A study on static and dynamic behavior of outrigger structural system for tall buildings, Bonfring international journal of industrial Engineering and Management Science, 2 (2012) 4, pp. 15-20

[19] ECP: ECP-201: Egyptian code for calculating loads and forces in structural work and masonry, Housing and Building National Research Center, Ministry of Housing, Utilities and Urban Planning, Cairo; 2008.

[20] Murty, C.V.R. et al.: Some concepts in earthquake behaviour of buildings, Gujarat State Disaster Management Authority, Government of Gujarat, 2012.

[21] BIS, I.: Indian Standard Plain and Reinforced Concrete-Code of Practice (4th Revision), Bureau of Indian Standards, New Delhi, 2000.